Proceedings of the Canadian Society for Mechanical Engineering International Congress
32nd Annual Conference of the Computational Fluid Dynamics Society of Canada
Canadian Society of Rheology Symposium
CSME-CFDSC-CSR 2025
May 25–28, 2025, Montréal, Québec, Canada

Investigating Automotive Sensor Perception in Rain: A Case Study on TOF and FMCW LiDAR

Long Li[1, 2*], Wing Yi Pao[1], Martin Agelin-Chaab[1], John Komar[2], Haoxiang Lang[1]
[1]Faculty of Engineering and Applied Science, Ontario Tech University, Oshawa, Canada
[2]ACE Climatic Aerodynamic Wind Tunnel, Ontario Tech University, Oshawa, Canada
*long.li@ontariotechu.net

Abstract—With the rise of automated features offered in modern and autonomous vehicles, it is essential to understand the capabilities and limitations of the perception systems to ensure safe maneuvers. One of the challenging conditions is operating under adverse weather as soiling occurs on vehicle surfaces and the adherent particles cause degradation in visibility. In this study, the performance of automotive Light Detection and Ranging (LiDAR) sensors when driving in rain is investigated. The study was carried out using a wind tunnel and a novel rain simulation system to produce realistic and controlled conditions. In particular, two types of LiDARs employing the time-of-flight (TOF) and coherent ranging principles (Frequency-modulated continuous wave – FMCW) were evaluated under various adverse driving and rain conditions. In addition, the effects of sensor cover material properties were parameterized based on surface wettability, which resulted in diverse droplet dynamics under the exposure of wind and raindrops. It was found that the TOF LiDAR had better transmittance when a layer of water film was formed on a hydrophilic cover but has caused poor FMCW LiDAR performance. In contrast, the TOF LiDAR was nearly blinded when there were large quantities of small and semi-spherical droplets present on a hydrophobic cover, for which the signal beams were scattered and deflected. However, the FMCW LiDAR was marginally influenced by the non-wetting scenarios. The potential causes of the difference in behaviors were examined by reviewing the mechanisms of the two types of LiDARs.

Keywords-LiDAR; sensor; FMCW; TOF; ADAS; autonomous vehicle; vehicle soiling; droplet dynamics; hydrophobicity; hydrophilicity; rain simulation; adverse weather; wind tunnel

I. INTRODUCTION

Advanced Driver Assistance Systems (ADAS) have introduced automated driving aids through the use of perception sensors, including cameras, LiDARs, RADARs, and ultrasonic sensors. These technologies enable powerful 3D mapping and spatial navigation by detecting and analyzing the surrounding environment. For instance, LiDAR sensors play a critical role in autonomy due to its ability to accurately detect object positions and being unaffected in low-light conditions.

While automation enhances precision and convenience, sensor performance is often compromised in adverse weather conditions. Time-of-flight (TOF) LiDAR degradation in rain has been reported in several studies [1, 2, 3], typically in the form of missing point clouds compared to dry conditions, as demonstrated in Fig. 1. In other words, fewer points are detected, leading to a reduction in visibility. However, frequency-modulated continuous-wave (FMCW) LiDAR performance in rain remains less understood compared to TOF LiDAR. This is likely due to its recent adoption in automotive LiDAR technology, as FMCW has traditionally been more prevalent in RADAR systems.

Given the limited data on FMCW LiDAR performance in adverse weather, rapid, realistic, and repeatable rain case

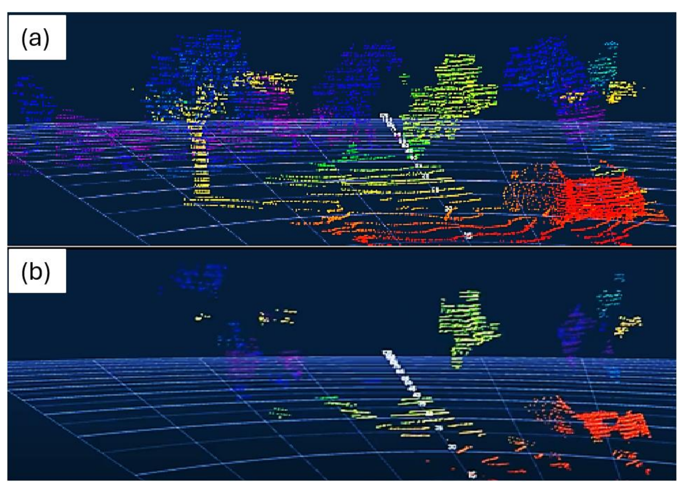

Figure 1. Examples of LiDAR vision in (a) dry, and (b) rain conditions.

studies on both TOF and FMCW LiDARs were conducted using the wind tunnel method outlined in [4].

This paper contributes to the field by benchmarking multiple critical parameters that influence autonomous vehicle perception in rainy conditions, including driving speeds, rain intensities, sensor surface material properties, and LiDAR operating principles. The data obtained from controlled and realistic rain testing will provide fundamental understanding of the interactions between these parameters that is beneficial for numerical and virtual modeling.

II. Literature Review

A. TOF and FMCW LiDARs

There are two ranging mechanisms known for LiDAR technology, namely pulsed and coherent ranging [5]. Pulsed LiDAR utilizes the TOF principle to obtain distance data based on the homodyne signal time delay. On the other hand, coherent ranging employs frequency modulation of a single light stream to obtain both distance and velocity data simultaneously by extracting the frequency and phase shift of the waves [6].

Although a TOF LiDAR may be simpler in construction and signal processing involved, it is prone to external interferences. FMCW LiDARs are believed to have closer performance as RADARs in adverse weather conditions with the capability to penetrate through obscuring media [7], however, the detection range is limited by its receiver bandwidth [8]. In general, a FMCW LiDAR uses less peak power than a conventional TOF LiDAR; it also offers advantages for better object recognition with higher sensitivity to the return wave [9]. Traditionally, TOF LiDARs have been widely adopted in the automotive industry and typically offers at 905 nm. However, TOF LiDARs are found to have limitations being prone to interferences, such as solar light and other nearby LiDAR units. It has been reported that shifting to 1550 nm can provide improvements over 905 nm to reduce detection noise and eye safety [10]. It is further believed that FMCW LiDARs will increase in their adoption given their advantages in lower laser power, higher sensitivity to photons, higher accuracy, unique signals encoded for the unit, and amplified signals.

B. Rain Dynamics

When driving, some surfaces experience more rain, known as the perceived rain intensity [11]. Besides amount of rain, the droplet size distributions are also found to have profound effects on sensor vision. Duration, size, and shape of raindrops adhering on the sensor surface are crucial parameters to sensor perception. Typical rainfall events have droplets around 1 mm in size, but the size is affected by winds and driving conditions; there may also be secondary soiling that brings tire spray from the vehicle in front.

These scenarios can be tested outdoors; however, outdoor testing often lacks repeatability due to uncontrolled variables. More controlled testing strategies were reported in the open literature, generally divided into two methods – driving through a static artificial rain zone or wind driven rain using a wind tunnel to bring the raindrops onto the stationary vehicle [11]. Traditionally, spray and sprinkler nozzle systems are used to produce the artificial raindrops, they are easy to control in bulk but sacrifice quality of rain simulated. Typical challenges include realistic droplet size and volume distributions where often there are large number of small droplets that are only suitable for secondary soiling. On the other hand, drop-forming systems using individual drip nozzles have modularity tuned for broad conditions but difficult to implement control strategies in large scale, thus requires scalable approach.

C. Materials Effects

Surface material properties can be classified based on their wettability to describe the equilibrium shape of a droplet with respect to the interfacial tensions of the liquid, air and solid phases [12]. Typically, hydrophilic materials have WCA $< 90^{o}$, hydrophobic materials have WCA $> 90^{o}$, and superhydrophobic materials exceed WCA of 150^{o}. The suitability of various materials for sensor cover application is often a debatable topic, which requires full characterizations with a broad range of materials and controlled testing, similar to our previous work reported in [3] for a TOF LiDAR.

Moreover, the type of sensors and the algorithms of signal processing may play significant roles in the data output. These occasions include when the return power of a TOF LiDAR is weakened due to part of the beam not returning to the receiver [13], or the multiple layers of FMCW signal filtering based on timing, frequency, and wavelength of the signals [14]. Nonetheless, it is still crucial to understand the consequent trends from the perspective of interactions between optics, materials, and droplet dynamics.

It was reported that a water film-forming hydrophilic material can retain LiDAR vision compared to a droplet-forming hydrophobic material under lighter rain conditions [3, 13]. This behavior can be treated as a single-beam problem and reasoned with Snell's law, for which droplets act as localized optical lenses that reflect and refract lights. To the authors' best knowledge, there is currently no comprehensive rain studies on FMCW LiDARs. Therefore, the objective of this paper is to evaluate the material effects on the performance of a FMCW LiDAR and compare it with a TOF LiDAR.

Figure 2. Model wind tunnel experimental setup, showcasing the model scale Vertical Rain Simulation Apparatus, and the sensor enclosure.

III. Methodology

This paper investigates the perception degradation of two types of automotive LiDAR sensors under driving-in-rain scenarios – FMCW and TOF. To achieve controlled, repeatable, and realistic soiling conditions, a wind-driven rain simulation system is used in a wind tunnel [4]. The system replicates vehicle-perceived rain while maintaining consistent aerodynamic influences showcased in Fig. 2.

The LiDAR sensors are enclosed in waterproof housings to maintain uniform aerodynamic conditions, protect the sensors from harsh environmental exposure, prevent unwanted external factors such as lens fogging that may introduce errors, and allow for external cover material variations without altering physical geometry. Due to size constraints in the wind tunnel test section, rain measurement and calibration are conducted using an optical disdrometer separately and before sensor enclosures are introduced. This method has demonstrated high repeatability in previous studies [15].

A. *Wind Tunnel Experimental Setup*

The experiments are conducted in a 1/14th scale open-loop wind tunnel at the ACE Climatic Wind Tunnel, Ontario Tech University, Canada. The push-down type design ensures that soiling particles such as water droplets are not reintroduced into the system. The test section measures 1.1 m in length, 0.5 m in width, and 0.4 m in height. To mitigate blockage effects, the test section walls are removed, and collector flaps are installed before the diffuser section.

LiDAR sensor enclosures are positioned at the center of the test section to ensure unobstructed airflow on all sides, preventing boundary layer buildup on the bottom wall. This setup maintains symmetrical frontal stagnation pressure distributions along both horizontal and vertical axes. Given the sensitivity of droplet dynamics in multiphase flow, this configuration minimizes aerodynamic effects that could alter droplet behavior on the enclosure surface while also preventing water accumulation at the bottom of the test section.

B. *Wind-driven Rain Experimental Simulation*

A Vertical Rain Simulation Apparatus (VeRSA) is used to generate realistic vehicle-perceived rain conditions by injecting water streams or droplets vertically into the horizontal wind stream. The system leverages droplet breakup and coalescence physics to simulate real-world rain events.

By varying the water flow rate and injection pressure, parameters such as nozzle exit velocity and flow regime are controlled, directly influencing the simulated rain characteristics at the target location. Previous studies have shown that optical sensor performance, including LiDAR and cameras, is highly sensitive to incoming rain characteristics [16]. Therefore, maintaining high similarity in rain intensity, droplet size distribution (DSD), and droplet volume distribution (DVD) is crucial for achieving realistic rain conditions.

Rain characteristics are measured using a Thies Laser Precipitation Monitor (LPM), an optical disdrometer that captures droplet size and velocity passing through a pre-defined laser plane. For each rain condition, continuous measurements are taken at one-minute intervals and repeated three times. The VeRSA system demonstrates good repeatability, with an average coefficient of variation (CV%) of 3.73%.

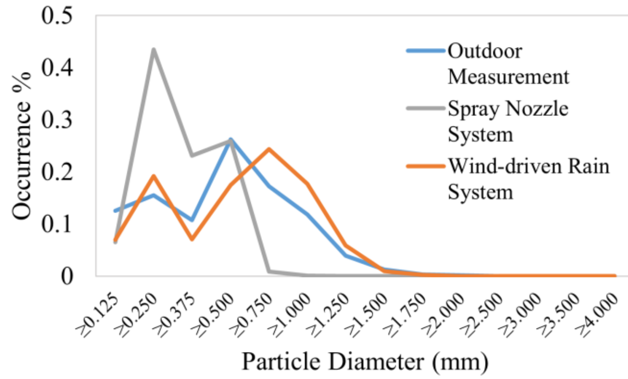

Figure 3. Droplet size distribution (DSD) comparison between traditional spray nozzle system, novel VeRSA system, and outdoor measurements.

Compared to traditional wind tunnel rain simulation methods, which rely on pressurized spray nozzles, the VeRSA system significantly improves realism in artificial rain conditions. A droplet size distribution comparison example is presented in Fig. 3. To validate its accuracy, experiments were conducted at the GM CTC MATT test facility in Oshawa, Canada, where simultaneous rain measurements were taken under dynamic on-vehicle and static weather station conditions [17]. These outdoor experiments not only provided a simulation reference but also validated the concept of perceived rain intensity, demonstrating that the rain intensity perceived by a moving vehicle is proportional to its velocity.

For this study, a matrix of nine cases is tested. Three rain intensities – light, moderate, and heavy – are tested at three wind speeds of 50 kph, 75 kph, and 100 kph representing city, sub-urban, and highway driving speeds, resulting in nine distinct rain conditions. The selected conditions cover a range from light drizzle to torrential rain, which includes considerations of showers that frequently occurs in short duration but extremely heavy and detrimental to driver and sensor visibilities. The rain condition test matrix is presented in Table 1.

C. *LiDAR Sensor Visibility Evaluation*

Two LiDAR sensors are evaluated – FMCW and TOF. Both sensors use the same detection target, a wind tunnel flow-conditioning honeycomb located in the settling chamber. This ensures that the detection target remains constant and unaffected by external factors. While FMCW and TOF LiDARs operate using different sensing principles, careful effort is made to minimize discrepancies caused by hardware and software settings.

For each rain condition, point cloud data is recorded for two minutes unless material degradation such as coating failure is observed. The raw point cloud data is processed to determine the total visible point cloud within the detection target region, with missing point cloud data representing visibility loss. LiDAR perception visibility is analyzed as a relative percentage

TABLE I. PERCEIVED RAIN CONDITION TEST MATRIX

Rain Condition	Wind Speed		
	50 kph	*75 kph*	*100 kph*
Light	23.1 mm/h	31.2 mm/h	79.0 mm/h
Moderate	50.5 mm/h	94.8 mm/h	284.2 mm/h
Heavy	132.5 mm/h	290.0 mm/h	801.2 mm/h

compared to a dry control frame and is mathematically represented as

$$\% \, Visibility = \frac{Point\ cloud\ count\ in\ rain}{Point\ cloud\ count\ in\ dry} \times 100\% \qquad (1)$$

Five different cover materials are tested with each LiDAR sensor. These covers vary in wettability, measured by their static water contact angles (WCA) at 16.7°, 57.1°, 81.9°, 107.8°, and 152.0°, which spans across different classes of materials – hydrophilic, moderately hydrophobic, hydrophobic, and superhydrophobic, respectively. While the increments across the full WCA range from 0° to 180° is uneven due to practical constraints in material preparation, these test cases provide valuable insight into how LiDAR performance changes with different surface properties.

IV. RESULTS AND DISCUSSION

In this study, we analyze the sensor performance results through two perspectives: 1) FMCW and TOF LiDAR visibility vs. incoming rain conditions, and 2) FMCW and TOF LiDAR visibility vs. water contact angle (WCA).

A. *TOF LiDAR Performance in Rain*

Fig. 4 presents the TOF LiDAR performance under varying rain intensities. The data reveals a negative correlation between LiDAR visibility and rain intensity; as rain intensity increases, visibility decreases. This degradation stems from complex interactions between LiDAR pulses and water droplets on the sensor cover.

When raindrops impact the LiDAR cover, they may coalesce with existing droplets, spread into a water film, bounce off the surface, or dislodge other droplets. These on-cover droplets are more influential than mid-air atmospheric droplets in degrading LiDAR performance. The on-cover droplets cause reflection, refraction, total internal reflection, scattering, and absorption of the LiDAR signals, leading to beam deflection and potential signal losses. Despite the unpredictability of these dynamic interactions, the overall trend indicates that higher rain intensities result in reduced LiDAR visibility.

While material property in terms of WCA is a key indicator of surface wettability, it doesn't fully capture all material properties affecting LiDAR performance. Factors not represented by WCA include surface energy distribution, which can vary locally and influence droplet behavior; surface

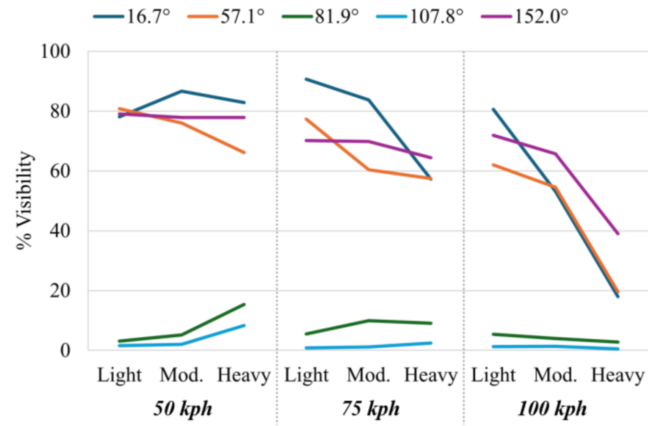

Figure 4. TOF LiDAR perception visibility under various wind-driven rain conditions with respect to different surface properties.

roughness and texture which affect droplet adhesion, movement, and dynamic wetting behaviors, as WCA measures static angles and doesn't account for hysteresis; and the tendency of some materials to form water films despite higher WCA, altering optical transmission. These factors contribute to the nonlinear relationship between LiDAR visibility and both rain intensity and material properties.

Nonetheless, WCA is still a suitable parameter for generalized description of the wettability and surface droplet dynamic trends for the study. The addition of hysteresis angles, such as advancing and receding angles, will be beneficial for modeling with larger datasets.

Notably, our results show a significant decline in LiDAR performance for hydrophobic covers with WCAs between 70° and 110°, where the LiDAR nearly goes blind. In contrast, hydrophilic and superhydrophobic covers maintain better performance. This phenomenon can be attributed to the behaviors of water droplets, such as size and shape on surfaces. For a TOF LiDAR, external flat medium that is thin and stable can retain signal transmission and receiving by only having small degree of refraction of the light pulses. In other words, majority of the beam can be returned. However, individual droplets act as localized lenses. The curvatures of the droplets cause refraction, reflection, and scattering to larger extent that cause beam to be loss and unable to be detected. As rain intensity increases, the amount of droplets present also increases, hence, more signal attenuation and visibility loss.

Surfaces with WCAs in the 70° to 110° range may promote the formation of stable droplets that adhere to the sensor cover, causing significant optical distortion. These droplets tend to be hemi-spherical and have large contact area that becomes stubborn for removal by wind via sliding motion. These droplets can obstruct or deflect the LiDAR signals more severely than on hydrophilic surfaces, where water tends to spread into a thin film, or superhydrophobic surfaces, where droplets bead up into more spherical shape and roll off quickly. The increased adhesion and stability of droplets on moderately hydrophobic surfaces lead to greater signal degradation, explaining the observed performance degradation in this WCA range.

B. *FMCW LiDAR Performance in Rain*

Fig. 5 illustrates the performance of FMCW LiDAR under varying rain intensities and wind speeds. Unlike TOF LiDAR, FMCW systems exhibit distinct responses to hydrophilic surfaces, especially those prone to forming water films. The data indicates that FMCW LiDAR experiences significant signal degradation when water films develop on hydrophilic sensor covers.

This degradation arises from the fundamental operating principles of FMCW LiDAR, which relies on the interference of continuous wave signals to determine distance and velocity. The presence of a water film on the sensor cover introduces a uniform medium that can alter the phase and frequency of the transmitted and received signals. This alteration leads to phase noise and frequency shifts, disrupting the interference pattern essential for accurate measurements. Consequently, the system may register false distances or velocities or even fail to detect objects altogether.

As wind speeds increase, particularly beyond 75 kph, the aerodynamic force on the sensor cover intensifies. This force flattens adhering droplets, promoting the formation of continuous water films. Such films exacerbate signal degradation in FMCW LiDAR systems, often leading to near-total loss of visibility. This effect is especially pronounced on hydrophilic surfaces, where water spreads easily, facilitating film formation.

In contrast, hydrophobic and superhydrophobic surfaces prevent water film formation due to lower surface energy, which cause droplets to bead and stay individual to help slide or roll off. On these surfaces, water remains as discrete droplets, which, while still present, have a less detrimental effect on FMCW LiDAR performance. The system maintains better functionality under increasing rain intensities because individual droplets cause less phase disruption compared to continuous films. The absence of a uniform medium means that the interference pattern of the FMCW signal remains largely intact, allowing for more reliable distance and velocity measurements.

FMCW LiDAR is seen to exhibit a similar failure mode to millimeter-wave (mmWave) radar, another key sensor in automotive ADAS applications. Both systems rely on continuous wave interference, making them largely unaffected by discrete droplets or snowflakes, as these do not significantly disrupt phase coherence. However, when a continuous medium forms, such as a water film on a LiDAR cover or a dense ice layer on a radar surface, signal propagation is fundamentally altered. The presence of a uniform layer increases attenuation, refraction, and phase distortion, effectively breaking the interference pattern required for accurate measurements. This is particularly evident in mmWave radar during heavy snowfall, where accumulated snow, compressed by aerodynamic forces, transitions into an ice sheet that disrupts signal penetration. In such conditions, adaptive cruise control (ACC) systems often fail, mirroring the loss of functionality seen in FMCW LiDAR when a water film forms.

C. *TOF and FMCW LiDAR Visibility vs. Water Contact Angle*

Fig. 6 compares TOF and FMCW LiDAR visibility across different water contact angles; the visibility scores presented in Fig. 6 are nine-condition-averaged. The trends reveal fundamental differences in how each LiDAR type responds to surface wettability when exposed to the same driving-in-rain conditions.

FMCW LiDAR exhibits the poorest performance on hydrophilic surfaces, where water films form readily. As WCA increases, indicating more hydrophobic surfaces, visibility improves significantly. Superhydrophobic surfaces (WCA > 150°) maintain high visibility, as water droplets bead up and roll off, preventing film formation. This behavior underscores FMCW LiDAR's sensitivity to phase distortions introduced by uniform water layers.

TOF LiDAR, however, shows different characteristics. Its performance deteriorates most on moderately hydrophobic surfaces (WCA between 70° and 110°), where droplets adhere without forming continuous films. These stable droplets cause scattering and refraction, leading to signal attenuation and

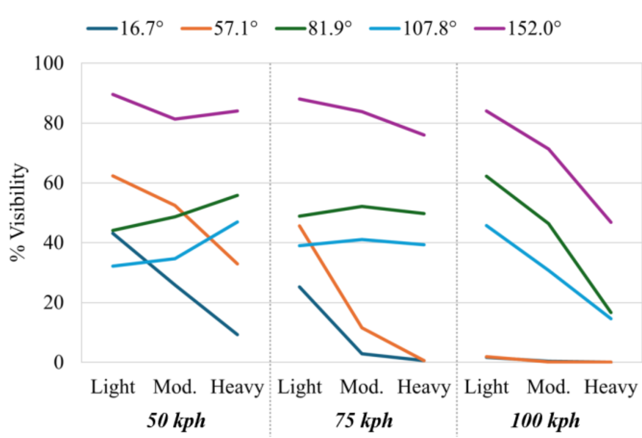

Figure 5. FMCW LiDAR perception visibility under various wind-driven rain conditions with respect to different surface properties.

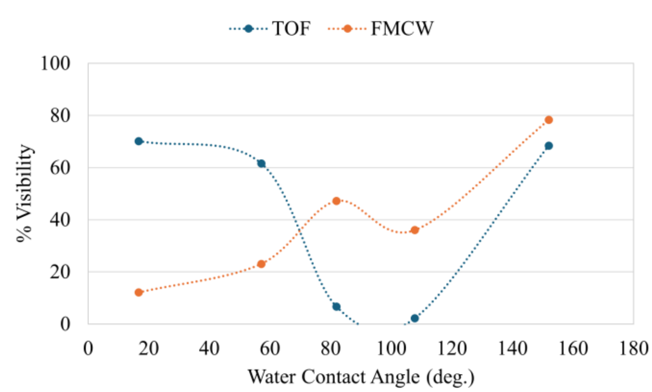

Figure 6. TOF and FMCW LiDAR averaged visibility across all rain conditions vs. water contact angle of cover surfaces.

reduced accuracy. Hydrophilic surfaces, which promote thin water films, and superhydrophobic surfaces, which facilitate rapid droplet shedding, both help maintain better TOF LiDAR performance. The uniformity of water films on hydrophilic surfaces causes consistent signal attenuation but less scattering, while superhydrophobic surfaces minimize droplet adherence, reducing optical distortions.

V. Conclusion

The increase in LiDAR sensor adoption in modern and autonomous vehicles has led to the need of understanding the performance of these sensors in various driving and weather conditions. This study investigated the performance degradation of frequency-modulated continuous-wave (FMCW) and time-of-flight (TOF) LiDAR sensors in when driving in rain through controlled wind tunnel experiments. Using a novel wind-driven rain simulation system, the effects of rain intensity, wind speed, and sensor cover materials over a broad range of realistic conditions were analyzed and discussed.

TOF LiDAR performance was found to decline with increasing rain intensity, primarily due to increasing on-cover droplet interactions affecting signal transmission. Moderately hydrophobic surfaces in the range of 70°-110° WCA led to the worst performance, where the individual droplets adhered have disrupted visibility through light refraction and scattering. In contrast, FMCW LiDAR was observed to be more sensitive to water films forming on hydrophilic surfaces, especially the ones with lower WCA, causing severe signal distortion. Both hydrophobic and superhydrophobic covers helped maintain visibility by preventing film formation. The results align with FMCW radar performance trends, where discrete droplets cause minimal disruptions, but a continuous medium leads to signal failure.

The findings emphasize the importance of sensor surface properties in maintaining LiDAR functionality in adverse weather, and their suitability for various types of sensors. Future work will focus on advanced modeling of droplet dynamics in multiphase flow scenarios, particularly in the context of automotive ADAS applications. A deeper understanding of critical parameters, such as rain-induced signal distortion and material interactions, will help define the limitations of current technology. This will guide future sensor development and mitigation strategies to improve perception reliability in rain. Ultimately increasing the level of autonomy, reducing accidents and contributing to safer road environments.

Acknowledgment

The authors acknowledge the financial support by the Natural Sciences and Engineering Research Council of Canada (NSERC), and the equipment support by Environment Canada.

References

[1] A. Carballo, J. Lambert, A. Monrroy, D. Wong, et al., “LIBRE: the multiple 3D LiDAR dataset,” IEEE Intelligent Vehicles Symposium (IV), October 2020.

[2] C. Linnhoff, K. Hofrichter, L. Elster, P. Rosenberger, and H. Winner, “Measuring the influence of environmental conditions on automotive lidar sensors,” Sensors, vol. 22, 5266, July 2022.

[3] W.Y. Pao, L. Li, M. Agelin-Chaab, L. Roy, et al., “Driving in the rain: evaluating how surface material properties affect LiDAR perception in autonomous driving,” SAE Technical Paper, 2025-01-8016.

[4] W.Y. Pao, L. Li, J. Howorth, M. Agelin-Chaab, et al., “Wind tunnel testing methodology for autonomous vehicle optical sensors in adverse weather conditions,” In: A.C. Kulzer, H.C. Reuss, A. Wagner (eds), 23. Internationales Stuttgarter Symposium, Springer Vieweg, Wiesbaden, 2023.

[5] Z. Wu, Y. Song, J. Liu, Y. Chen, et al., “Advancements in key parameters of frequency-modulated continuous-wave light detection and ranging: a research review,” Applied Sciences, vol. 14, 7810, 2024.

[6] J. Zheng, Optical frequency-modulated continuous-wave (FMCW) interferometry, Springer, New York, USA, 2005.

[7] A.M. Wallace, A. Halimi, and G.S. Buller, “Full waveform LiDAR for adverse weather conditions,” IEEE Transactions on Vehicular Technology, vol. 69, no. 7, July 2020.

[8] C. Zhang, T. Nagata, M.S.B.A. Sharifuddin, F. Ito, et al., “Long-range frequency-modulated continuous-wave LiDAR employing wavelength-swept optical frequency comb,” Optics Communications, vol. 545, 129702, June 2023.

[9] J. Riemensberger, A. Lukashchuk, M. Karpov, W. Weng, et al., “Massively parallel coherent laser ranging using a soliton microcomb,” Nature, vol. 581, pp. 164-170, May 2020.

[10] P. McManamon, Field Guide to Lidar, SPIE Field Guides, vol. FG36, J.E. Greivenkamp (Ed), SPIE Press, Bellingham, Washington, USA, 2015.

[11] W.Y. Pao, M. Carvalho, F. Hosseinnouri, L. Li, et al., “Evaluating weather impact on vehicles: a systematic review of perceived precipitation dynamics and testing methodologies,” Engineering Research Express, vol. 6, 013001, 2024.

[12] G. McHale, M.I. Newton, and N.J. Shirtcliffe, “Water-repellent soil and its relationship to granularity, surface roughness and hydrophobicity: a materials science review,” European Journal of Soil Science, vol. 56, p. 445-452, 2005.

[13] W.Y. Pao, J. Howorth, L. Li, M. Agelin-Chaab, et al., “Investigation of automotive LiDAR vision in rain from material and optical perspectives,” Sensors, vol. 24, 2997, May 2024.

[14] Aurora, “FMCW lidar: the self-driving game-changer,” April 2020, online, available at https://blog.aurora.tech/engineering/

[15] W.Y. Pao, L. Li, and M. Agelin-Chaab, "A Method of Evaluating ADAS Camera Performance in Rain - Case Studies with Hydrophilic and Hydrophobic Lenses," presented at the Canadian Society for Mechanical Engineering International Congress, Sherbrooke, QC, Canada, May 28-31, 2023, 2023.

[16] L. Li, W.Y. Pao, M. Agelin-Chaab, and J. Komar, "From Raindrops To Pixels: A Novel Model to Predict ADAS Camera Image Degradation in Rain," presented at the 2024 IEEE International Conference on Smart Mobility (SM), Niagara Falls, ON, 2024.

[17] W.Y. Pao *et al.*, "Perceived Precipitation Intensity Prediction Model Based on Simultaneous Dynamic and Static Observations for Evaluating Weather Impacts on Vehicle Applications," *Journal of Traffic and Transportation Engineering (English Edition)*, p. 20, 2024. In press.